electronic materials

MDPI

Article

The Extraction of the Density of States of Atomic-Layer-Deposited ZnO Transistors by Analyzing Gate-Dependent Field-Effect Mobility

Minho Yoon

Department of Physics and Institute of Quantum Convergence Technology, Kangwon National University, Chuncheon 24341, Republic of Korea; minhoyoon78@gmail.com

Abstract: In this study, we investigated the density of states extraction method for atomic-deposited ZnO thin-film transistors (TFTs) by analyzing gate-dependent field-effect mobility. The atomic layer deposition (ALD) method offers ultra-thin and smooth ZnO films, but these films suffer from interface and semiconductor defects, which lead to disordered localized electronic structures. Hence, to investigate the unstable localized structure of ZnO TFTs, we tried to derive the electronic state relationship by assuming field-effect mobility can be expressed as a gate-dependent Arrhenius relation, and the activation energy in the relation is the required energy for hopping. Following this derived relationship, the DOS of the atomic-deposited ZnO transistor was extracted and found to be consistent with those using temperature-dependent measurements. Moreover, to ensure the proposed method is reliable, we applied methods for the extraction of DOSs of doped ZnO transistors, which show enhanced mobilities with shifted threshold voltages, and the results show that the extraction method is reliable. Thus, we can state that the mobility-based DOS extraction method offers practical benefits for estimating the density of states of disordered transistors using a single transfer characteristic of these devices.

Keywords: localized trap states; field-effect mobility; thin-film transistors

Citation: Yoon, M. The Extraction of the Density of States of Atomic-Layer-Deposited ZnO Transistors by Analyzing Gate-Dependent Field-Effect Mobility. *Electron. Mater.* **2024**, *5*, 239–248. https://doi.org/10.3390/electronicmat5040016

Received: 1 August 2024
Revised: 19 September 2024
Accepted: 17 October 2024
Published: 19 October 2024

1. Introduction

Oxide semiconductor-based thin-film transistors (TFTs) have been extensively studied and widely used for electronic and optoelectronic applications because of their high electrical performance, uniformity, and low-cost device fabrication at relatively low temperatures [1–3]. Indeed, oxide thin-film transistors (TFTs) by atomic layer deposition (ALD) have been an emerging technology, as thin films by ALD can be downscaled to a nanometer scale due to layer-by-layer deposition characteristics [4,5]. However, ALD oxide thin films also suffer from interface and semiconducting defects, as do those by conventional deposition methods, such as sputtering and evaporation [4]. Due to these defects, the electronic structures of the semiconductors are localized, thereby resulting in the degradation of the electrical properties of these devices [6,7]. Thus, to enhance the electrical properties of these devices, it is essential to understand and analyze the electronic structures of the semiconductors. Hence, several approaches have been proposed, such as exploring defect states with hard X-ray photoelectron spectroscopy [8,9], calculating localized states using density functional calculations [10,11], characterizing defect states by illuminating with lights [12,13], and investigating trap-limited charge conduction states by exploring low-temperature conduction characteristics [4,14,15]. While there has been progress, these approaches often require relatively stable devices. If electrical characteristics change during measurements, those results can lead to misinterpreted consequences. Hence, the electronic structure analysis method, which is simple and applicable to unstable semiconductors, is highly required.

This study explored the density of states extraction method for atomic-deposited ZnO transistors. The self-limiting and layer-by-layer atomic deposition (ALD) methods offer ultra-thin and flat ZnO films and an n-type transistor operation with a field-effect mobility of 3.1 $cm^2V^{-1}s^{-1}$ [16–18]. However, thin-film analyses, such as X-ray photoelectron spectroscopy (XPS) and X-ray diffraction (XRD), show that deposited ZnO films are Zn-deficient polycrystalline structures. In addition, device parameters, such as the threshold voltage (*Vth*) and subthreshold swing (*S.S*), are arbitrary [19]. These non-ideal behaviors are due to the localized structure of ZnO from the defects [20,21]. Hence, to investigate the electronic structure of disordered ZnO film, we derived the density of states (DOS) in terms of gate-dependent field-effect mobility by modeling the field-effect mobility as a gate-dependent Arrhenius equation [22,23]. Following this relation, we extracted the DOS of ZnO TFTs from the single transfer curve, which was consistent with that obtained from low-temperature measurements. Indeed, to ensure the method for other semiconductors, we applied this method to analyze Al_2O_3-coated ZnO TFTs, which showed a shift in threshold voltage (*Vth*) and enhanced mobilities. Notably, DOSs from both methods showed similar distributions within an order. Thus, we concluded that the mobility-based extraction method would provide practical benefits for extracting the DOS of disordered localized transistors, as it can be estimated from a single transfer characteristic.

2. Materials and Methods

Bottom-gate top-contact (BGTC) ZnO TFTs were fabricated as shown in the optical microscope image in Figure 1a. A 10 nm-thin Al_2O_3-coated 200 nm-thick p^+-Si/SiO_2 wafer was used as the substrate, and a 6 nm-thin ZnO film was deposited by cyclic atomic layer deposition (ALD) at 80 °C using diethylzinc (DEZ, Aldrich, St. Louis, MO, USA) and water as zinc and oxygen precursors, respectively. After patterning the ZnO layer by a conventional lift-off process, a 50 nm-thick Al source and drain electrodes were deposited by thermal evaporation and patterned using a shadow mask, which had a width and length of 1000 and 360 μm, respectively. In addition, for the fabrication of Al_2O_3-coated ZnO TFTs, the top $A_{l2}O_3$ layer was also deposited by cyclic atomic layer deposition (ALD) at 110 °C using trimethylaluminum (TMA, Aldrich, St. Louis, MO, USA) and water as aluminum and oxygen precursors, respectively. The geometric capacitance of the dielectric was measured to be 16.4 nF cm^{-2} at 1 kHz, using an LCR meter (HP4284A, Agilent Technologies, Santa Clara, CA, USA). The thickness of these films was measured with an ellipsometer (AutoEL-II, Rudolph Research, Hackettstown, NJ, USA) and confirmed with an atomic force microscope (XE100, Park Systems, Suwon, Republic of Korea). The chemical state and composition of ZnO films were probed using X-ray photoelectron spectroscopy (XPS) with Al Kα (1486.6 eV) radiation, and recorded data was calibrated using the C-1 s spectrum with a binding energy of 284.6 eV (K-Alpha+, Thermo Fisher Scientific, Waltham, MA, USA). The stoichiometry of ZnO films was determined using the atomic sensitivity factors of 2.881 (Zn) and 31.861 (O), provided by Thermo Fisher Scientific Avantage© software (software version 5.984) and its ALTHERMO1 library. A homemade Hall measurement system was used to analyze ZnO films; an electromagnet (up to 1 T) was placed beneath the probing stage, and electrical signals were recorded with the semiconductor parameter analyzer (Model HP4155C, Agilent Technologies, Santa Clara, CA, USA). The current–voltage (*I*–*V*) characteristics of the transistors were investigated with a semiconductor parameter analyzer (Model HP4155C, Agilent Technologies, Santa Clara, CA, USA). A liquid-nitrogen cooling cryostat was used for temperature-variable current-voltage measurements. The temperature range was from 180 to 300 K. The field-effect mobility of the TFTs in a linear regime was estimated as the following equation

$$\mu_{lin} = \frac{1}{C_i V_{ds}} \frac{L}{W} \frac{\partial I_{ds}}{\partial V_{gs}} \quad (1)$$

where I_{ds} is the drain current, V_{gs} is the gate voltage, C_i is the geometric dielectric capacitance, V_{ds} is the drain voltage, and L and W are the channel length and width, respectively.

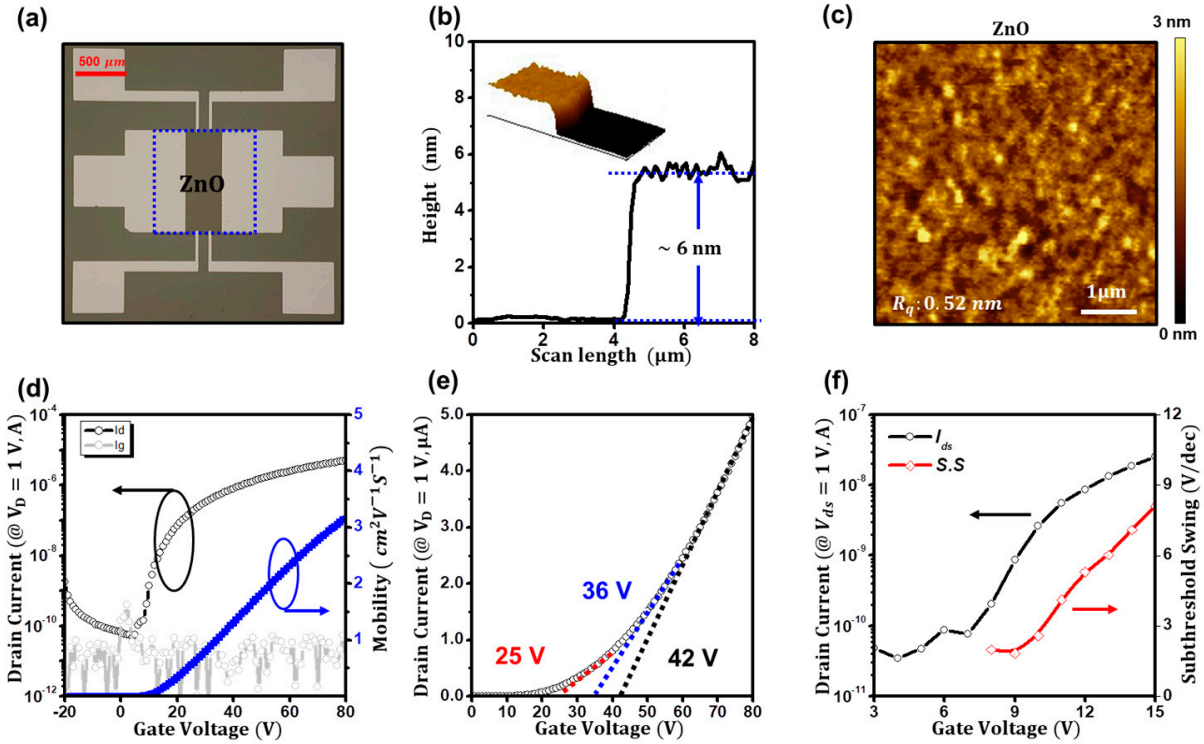

Figure 1. (**a**) Optical microscopy image of ZnO TFTs; (**b**) thickness profiles of ZnO film by AFM (inset: topographic image of ZnO layer); (**c**) surface morphology of ZnO film; (**d**) transfer characteristics (I_{ds} vs. V_{gs}) of ZnO TFTs; (**e**) threshold voltage extraction of ZnO TFTs with gate bias ranges up to 40 (red), 60 (blue), and 80 V (black); and (**f**) subthreshold swing of ZnO TFTs.

3. Results

Due to the self-limiting and layer-by-layer deposition characteristics of the atomic layer deposition method (ALD), the deposited ZnO film shows ultra-thin and flat thin-film characteristics: the thickness of the ZnO film was ~6 nm by atomic force microscopic (AFM) measurements, as shown in Figure 1b, and its surface roughness was ~0.5 nm without any discontinuity, as shown in Figure 1c. In addition, as shown in Figure 1d, atomic-deposited ZnO TFTs exhibit typical n-type transistor operation, of which the field-effect mobility from the transconductance is 3.1 $cm^2V^{-1}s^{-1}$ along with a high on/off ratio (>10^4). However, the threshold voltage (*Vth*) and subthreshold swing (*S.S*) are arbitrary, as shown in Figure 1e,f. The threshold voltage, estimated by the widely used linear fitting method, was 25 V when extracted up to the gate bias of 40 V. However, it increased to 36 and 42 V when extracted up to the gate bias of 60 and 80 V, respectively. Similarly, the subthreshold swing of ZnO TFTs was 1.8 V/dec at V_{gs} = 9 V. However, as the gate bias increased, it significantly increased to 5.3 V/dec at V_{gs} = 12 V, reaching 8.1 V/dec at V_{gs} = 15 V. These non-ideal transistor behaviors were due to interface and semiconductor defects [19]. Hence, we performed chemical and electronic analyses. The corresponding output curve for ZnO TFTs is shown in Figure S1.

Figure 2a shows the X-ray photoelectron spectroscopy (XPS) spectrum of the ZnO film. The Zn 2p peaks show the spin-orbit transition of Zn $2p_{1/2}$ and $2p_{3/2}$, which appeared at 1045.1 and 1021.9 eV, respectively. In addition, the O 1s peaks displayed mixed spectra, which could be resolved into the low-energy peak (O_I) at 530.5 eV, which corresponded to the O_2^- from the wurtzite structure of the ZnO lattice, and the high-energy peak (O_{II}) at 532.1 eV, which was from the oxidation of the surface when exposed to the air [24,25]. In addition, the stoichiometry of Zn to O of the film was 0.77, which indicates the non-stoichiometric Zn-deficient film was formed by ALD. Moreover, X-ray diffraction (XRD) analyses, as shown in Figure 2b, show that the ZnO film was a polycrystalline structure, of which crystallographic orientations of the (002) direction (34.50°) as well as

the (103) direction (55.37°) were shown in its spectra [26,27]. Please note that the survey spectrum of the ZnO film is shown in Figure S2. The electronic properties of metal oxide semiconductors are significantly dependent on chemical states and metal-to-oxygen stoichiometry [20]. Thus, due to the defective structure, the electronic structure of the ZnO film was strongly localized. Hence, to investigate the electronic structure of the ZnO film, we performed temperature-dependent current-voltage analyses of the TFTs. Figure 2c displays the temperature-dependent transfer characteristics of ZnO TFTs from 180 to 300 K. As the temperature rose, the drain current increased. By modeling the drain current with the Meyer–Neldel rule of $I(V_{gs}) = I_0\ exp(-E_a/kT)$ [28,29] and assuming the gate-dependent activation energy (E_a) as the energetic difference between the Fermi level and conductive states, the areal density of states, DOS, $g(E)$ could be deduced using the relation of $g(E) = qC_i\ (dE_a/dV_{gs})^{-1}$ [14]. Figure 2d displays the extracted density of states of ZnO TFTs. As forecasted, Figure 2d shows the tail-type localized energy distribution. In addition, using a Gaussian DOS model [30], $g(E) = N\sigma^{-1}2\pi^{-1/2}\ exp(-(E - E_c)^2/(2\sigma^2))$, where σ is the width of the distribution, N is the total concentration of the charge traps, and E_c is the position of the center of the peak, the total concentration of the charge traps and the width of the distribution were estimated as 6.7×10^{15} states cm^{-2} and 41 meV, respectively. This low-temperature DOS extraction method offered clear and conclusive results regarding the electronic states of the semiconductors. However, if the electrical characteristics of TFTs severely change during the measurements, the low-temperature method cannot be applied. In some sense, an in-depth study of the electronic structure of unstable semiconductors would be required more than it would be for stable semiconductors. For this reason, we tried to establish the extraction method using a single transfer characteristic. Please note that ZnO TFTs were stable enough to perform the repetitive low-temperature current-voltage measurements as the stable operation to the bias stress, as shown in Figure S3.

Charges in disordered semiconductors transport through thermally activated hopping [21]. Consequently, the field-effect mobility (μ) can be represented by an Arrhenius equation, as shown in Equation (2) [22]. By supposing the activation energy of E_a is a gate-dependent factor and identical to the activation energy from the Meyer–Neldel rule, the density of states can be derived with the gate bias-dependent field-effect mobility in Equations (3)–(5). Moreover, the activation energy can be determined from the integral of the deduced differential of the activation energy, of which the constant of the activation energy (E_0) can be deduced by assuming the lowest energy plus Boltzmann energy at room temperature (K_bT), as in Equation (6).

$$\mu = \mu_0 \exp\left\{-\frac{E_a(V_g)}{k_bT}\right\} \tag{2}$$

$$\ln\mu = \ln(\mu_0) - \frac{E_a(V_g)}{k_bT} \tag{3}$$

$$\frac{dE_a(V_g)}{dV_g} = -k_bT\frac{d\ln\mu}{dV_g} \tag{4}$$

$$g(E) = \frac{C_i}{q}\left(\frac{dE_a(V_g)}{dV_g}\right)^{-1} = -\frac{C_i}{qk_bT}\left(\frac{d\ln\mu}{dV_g}\right)^{-1} \tag{5}$$

$$E_a(V_g) = -k_bT\int_{V_t}^{V_g} E_a'(V_g)\ dV_g + E_0 \tag{6}$$

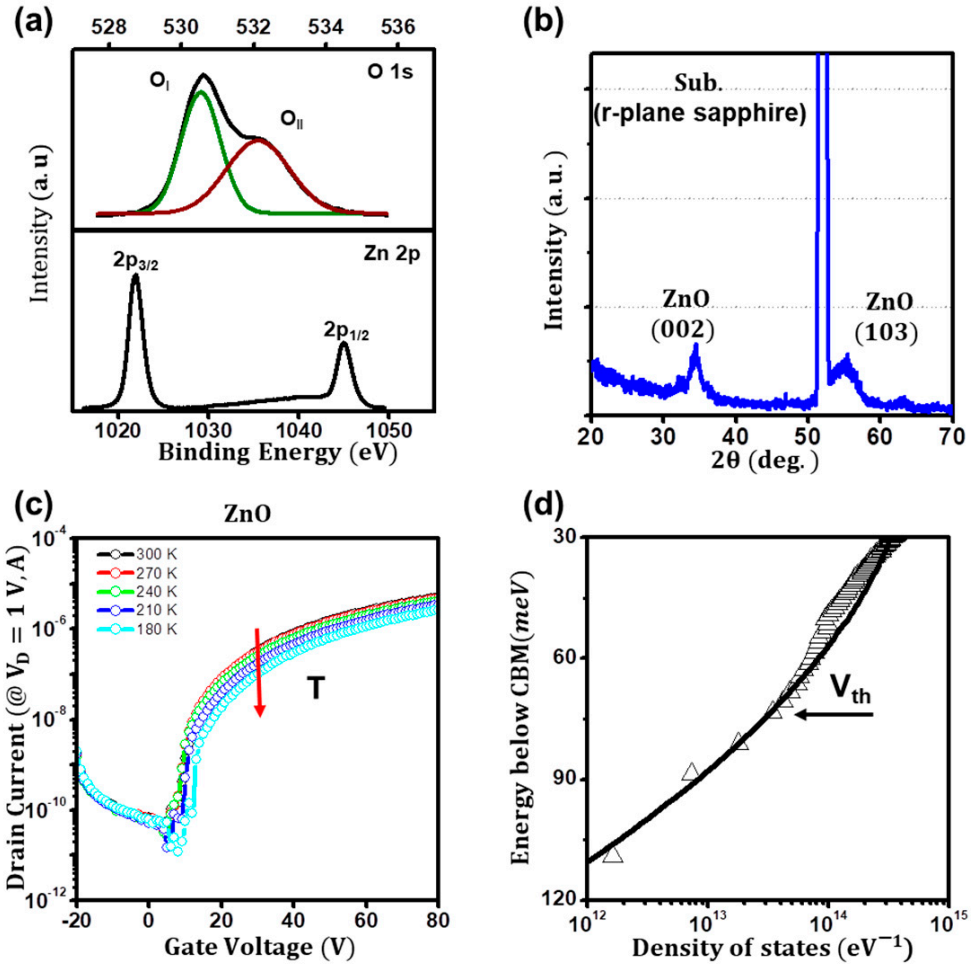

Figure 2. (**a**) XPS spectra of ZnO film; (**b**) XRD pattern of ZnO films; (**c**) temperature dependence of transfer curves of ZnO TFTs; and (**d**) extracted trap density of states (DOS) of ZnO TFTs.

Figure 3a,b show the mobility-based DOS estimation plots of ZnO TFTs. By differentiating the natural logarithmic field-effect mobility, the derivative of activation energies as a function of the gate voltage was obtained. Next, by fitting the integral of the derivative activation energies with an exponential decay function, the constant of the activation energy (E_0) was estimated, which was 0.102 eV. Next, using Equation (4), the DOS of ZnO TFTs was extracted, as shown in Figure 3c. Surprisingly, the observed DOS from mobility analyses was consistent with that from low-temperature analyses. At an energy below 60 meV, the densities of states from both methods were 10^{13} states eV^{-1}, and at an energy of 30 meV, they were ~10^{14} states eV^{-1}. Thus, we believed that the mobility-based extraction method was simple and beneficial. However, it was still doubtful whether this method applies to other disordered semiconductor-based TFTs. Hence, we fabricated Al_2O_3-coated ZnO TFTs and tried to ensure the approach. Please note that, probably due to the diffusion current effect, the density of states (DOS) obtained from the low-temperature measurement may appear slightly higher than that obtained from the mobility method, especially near the threshold voltage. However, the difference is negligible if the gate voltage is high enough.

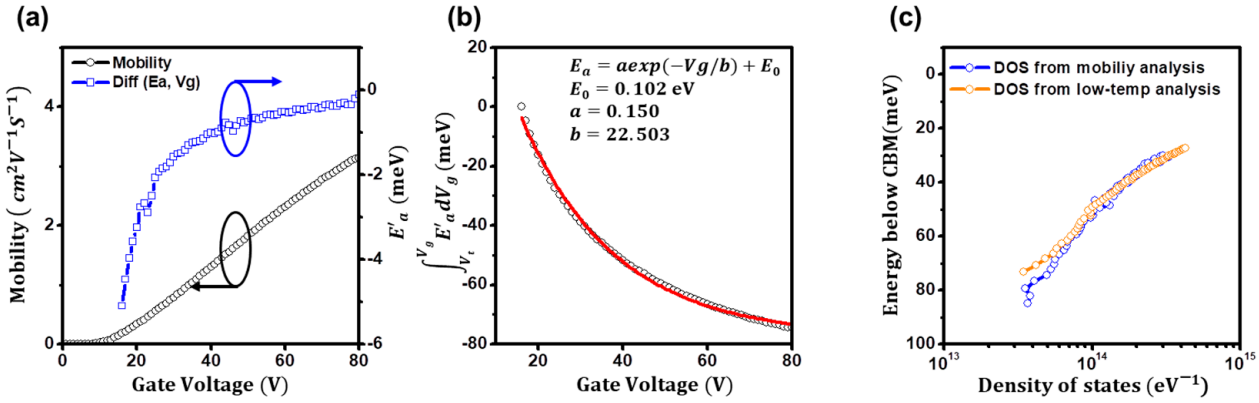

Figure 3. (**a**) Mobility-based DOS estimation plots of ZnO TFTs; (**b**) resulting activation energy from integral of derivative activation energies; and (**c**) extracted trap density of states (DOS) of ZnO TFTs.

Figure 4a,d show the transfer characteristics (I_{ds} vs. V_{gs} at V_{ds} = 1 V) of 1 and 3 nm-thin Al_2O_3-coated ZnO TFTs, respectively. The threshold voltage of the TFTs shifted, which was determined by 9 and −53 V for 1 and 3 nm-thin Al_2O_3-coated ZnO TFTs, respectively, using the modified extraction method of I_{ds}/g_m [19]. In addition, field-effect mobilities improved to 3.9 and 7.1 $cm^2V^{-1}s^{-1}$ for these TFTs, respectively. These massive changes in the electrical characteristics of ZnO TFTs were attributed to doping effects from the top Al_2O_3 layer. Aluminum (Al^-) and hydrogen (H^-) ions are known as effective electron doping agents for ZnO films [4,18,20]. Hence, if an Al_2O_3 layer is deposited on a ZnO layer, the ions diffuse, resulting in conductive changes in the ZnO film and threshold voltage shifts of the TFT. Next, we tried to extract the electronic structures of the Al_2O_3-coated ZnO TFTs using both methods, as shown in Figure 4b,e. Figure 4c,f show the DOSs of TFTs by both methods. As in the case of ZnO TFTs, the DOSs of TFTs from both methods were consistent within an order. At an energy below 60 meV, the densities of states from both methods were 10^{14} states eV^{-1}, and at an energy of 30 meV, they were close to 10^{15} states eV^{-1}. In addition, we attempted to analyse data using a Pearson similarity analysis method by selecting data presented in Table S1. The Pearson correlation coefficients were 0.998, 0.991, and 0.995 for ZnO and 1 and 3 nm-thin Al_2O_3-coated ZnO TFTs, respectively. Thus, the coefficients of determination were 0.997, 0.982, and 0.911 for these devices. A coefficient of determination of 1 indicated that the regression predictions perfectly fit these data. As a result, we believe that DOSs of ZnO TFTs determined by the mobility method were consistent with those determined by the low-temperature method. Thus, based on these experiments and findings, we can state that the mobility-based DOS extraction method is simple, reliable, and beneficial for in-depth analyses of the electronic structure of disordered semiconductors, as it can be obtained from a single transfer measurement. The temperature-dependent transfer characteristics of Al_2O_3-coated ZnO TFTs from 180 to 300 K are depicted in Figure S4, and surface morphologies of Al_2O_3-coated ZnO films are shown in Figure S5. Please note that the adjusted R-squared values of the activation fitting process in Figures 3b and 4b,e were estimated to be over 0.99. A value of one indicates a model that perfectly predicts values in the target field. Therefore, we consider the process to be reliable.

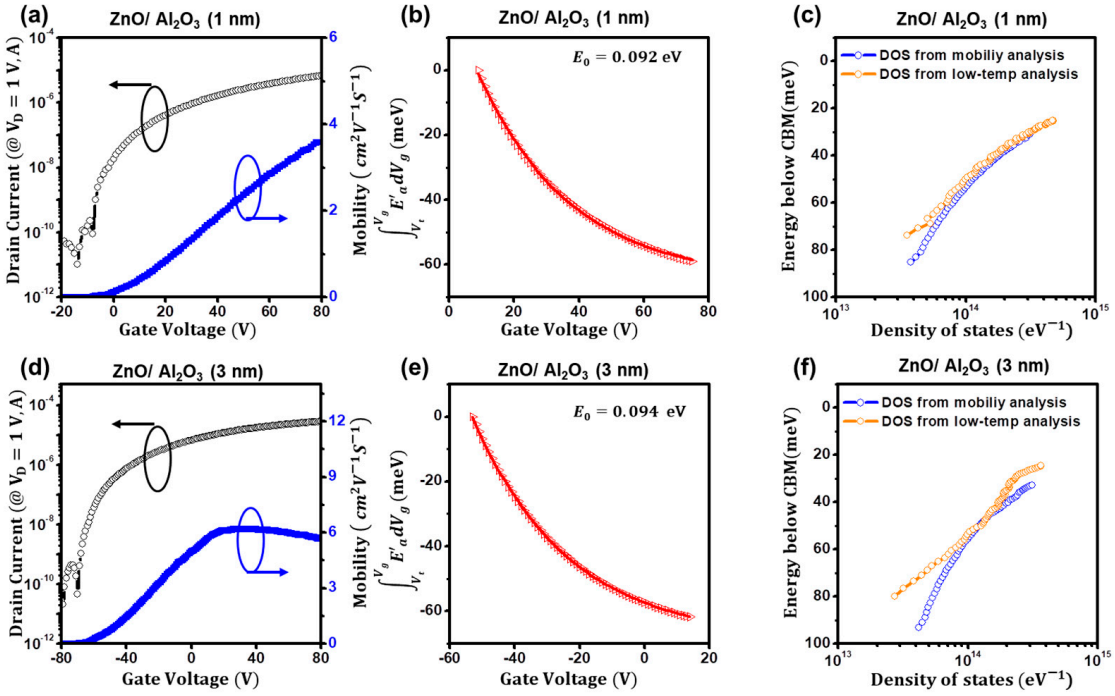

Figure 4. (**a**,**d**) Transfer characteristics (I_{ds} vs. V_{gs} at V_{ds} = 1 V) of 1 and 3 nm-thin Al_2O_3-coated ZnO TFTs, respectively; (**b**,**e**) mobility-based DOS estimation plots of 1 and 3 nm-thin Al_2O_3-coated ZnO TFTs, respectively; and (**c**,**f**) extracted trap density of states (DOS) of ZnO TFTs.

4. Discussion

We tried to understand the mobility enhancements in Al_2O_3-coated ZnO TFTs. As shown in Figure 5a, the mobility of Al_2O_3-coated ZnO TFTs showed higher values than that of ZnO TFTs. At the gate overdrive voltage of 60 V, the field-effect mobility was 2.9 $cm^2V^{-1}s^{-1}$ for ZnO TFTs, but it increased to 3.2 and 5.4 $cm^2V^{-1}s^{-1}$ for the 1 and 3 nm-thin Al_2O_3-coated ZnO TFTs, respectively. These improvements in mobility were due to doping effects, which might have led to decreases in the trap density of states and resulted in less-hindered charge transports. The carriers increased by doping filled the trap states, leading to a charge–transport transition from trap-limited conduction to percolation transport across the device channel [31,32]. However, as seen in Figure 5b, the DOSs of undoped and doped ZnO showed similar distributions above the threshold voltage, which means the doping effects on the DOSs of ZnO films were negligible. However, the mobility prefactor (μ_0) in Equation (2) seems the most evident among the TFTs shown in Figure 5c, which was 9.8 $cm^2V^{-1}s^{-1}$ for ZnO TFTs, while it was 11.1 and 20.6 $cm^2V^{-1}s^{-1}$ for 1 and 3 nm-thin Al_2O_3-coated ZnO TFTs, respectively. The mobility prefactor was affected by the wave function overlap between neighboring hopping sites, which was exponential in the distance between hopping sites according to hopping theory [33]. The Hall measurements in Figure 5d show that, through doping, the carrier concentration of Al_2O_3-coated ZnO films rose from ~10^{15} to ~10^{19} cm^{-3}, and the corresponding resistivity decreased from ~10^4 to ~10^{-1} ohm-cm. More study is necessary for an in-depth understanding of the charge transport of disordered semiconductors [34–36]. Nevertheless, we can now state that the dopants in the ZnO matrix might act as a bridge for hopping, thereby increasing the hopping probability and leading to enhanced mobilities, as shown in Figure 5e.

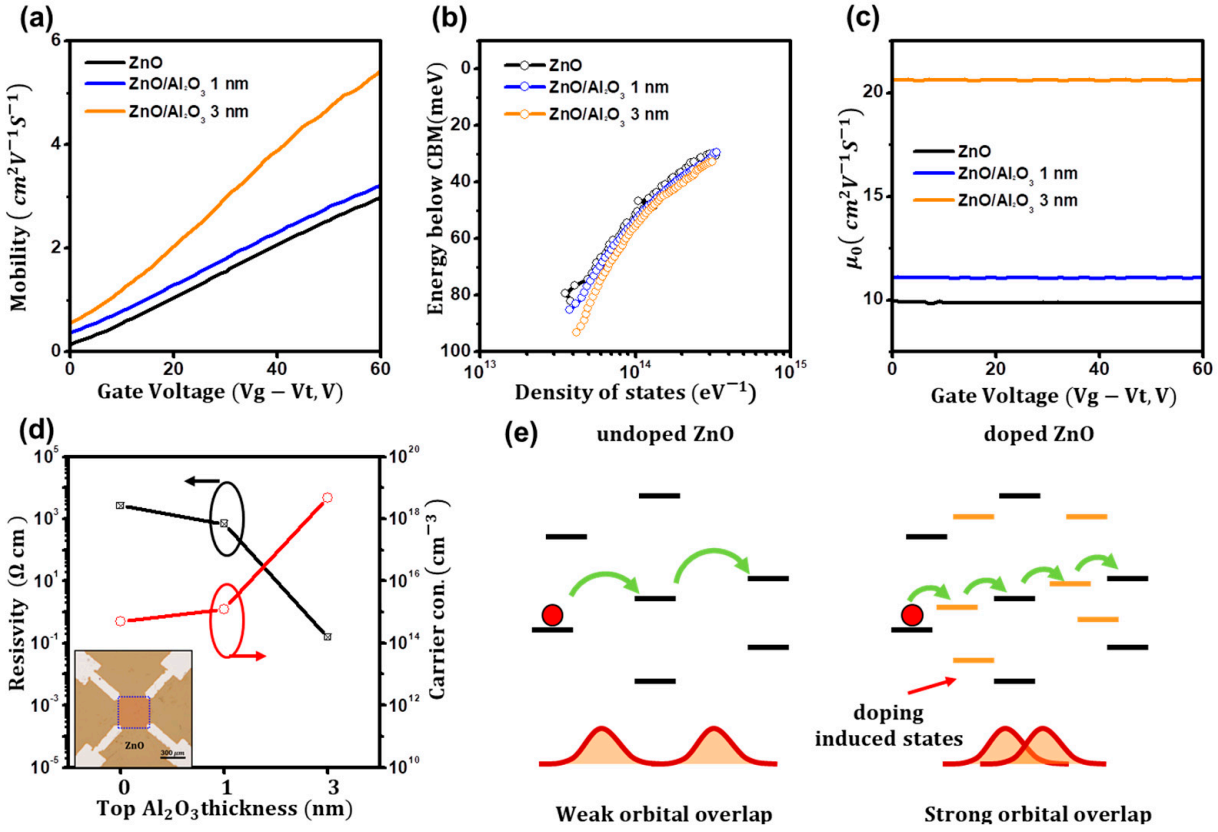

Figure 5. (**a**) Field-effect mobilities of pure and doped ZnO TFTs; (**b**) extracted trap density of states (DOSs) of TFTs; (**c**) mobility prefactors of pure and doped ZnO TFTs; (**d**) Hall measurements of pure and doped ZnO films (inset: optical microscope image of van der Pauw samples); and (**e**) schematic illustration of doping effects in ZnO films.

5. Conclusions

In this study, we proposed the density of states extraction method from a single transfer characteristic of disordered ZnO transistors. The density of states of disordered semiconductors is inversely proportional to the derivation of the gate-dependent activation energy; therefore, differentiating the natural logarithmic field-effect mobility as a function of gate voltage leads to the density of states. To ensure this mobility-based extraction method, the density of states of the atomic-deposited ZnO transistor was extracted and found to be consistent with temperature-dependent measurements. Moreover, to ensure the proposed method is applicable, we applied methods to extract DOSs of Al_2O_3-coated ZnO TFTs, and the results showed that the extraction method is reliable. Thus, we can state that the mobility-based DOS extraction method offers practical benefits for estimating the density of states of disordered transistors using a single transfer characteristic of these devices.

Supplementary Materials: The following supporting information can be downloaded at: https://www.mdpi.com/article/10.3390/electronicmat5040016/s1, Figure S1: Output curve of ZnO TFTs; Figure S2: Survey spectrum of ZnO films; Figure S3: Positive bias stress effect of ZnO TFT; Figure S4: Temperature-dependent transfer characteristics of 1 and 3 nm Al_2O_3-coated ZnO TFTs; Figure S5: Surface morphologies of 1 and 3 nm Al_2O_3-coated ZnO TFTs; and Table S1: Statistical analysis of extraction methods for the density of states of ZnO TFTs.

Funding: The author acknowledges financial support from the Basic Science Research Program (Sejong Fellowship) through the National Research Foundation of Korea (NRF) funded by the Ministry of Education (NRF-2022R1C1C2008865).

Data Availability Statement: Data presented in this study are available on request from the corresponding author.

Conflicts of Interest: The author declares no conflicts of interest.

References

1. Kim, S.; Kwon, H.J.; Lee, S.; Shim, H.; Chun, Y.; Choi, W.; Kwack, J.; Han, D.; Song, M.; Kim, S.; et al. Low-Power Flexible Organic Light-Emitting Diode Display Device. *Adv. Mater.* **2011**, *23*, 3511–3516. [CrossRef] [PubMed]
2. Rogers, J.A.; Someya, T.; Huang, Y. Materials and Mechanics for Stretchable Electronics. *Science* **2010**, *327*, 1603–1607. [CrossRef] [PubMed]
3. Xu, R.P.; Li, Y.Q.; Tang, J.X. Recent Advances in Flexible Organic Light-Emitting Diodes. *J. Mater. Chem. C* **2016**, *4*, 9116–9142. [CrossRef]
4. Yoon, M.; Hyun, D.; Kim, H.S. Subgap States in Aluminium- and Hydrogen-Doped Zinc-Oxide Thin-Film Transistors. *J. Mater. Chem. C* **2023**, *11*, 9952–9959. [CrossRef]
5. Tseng, R.; Wang, S.T.; Ahmed, T.; Pan, Y.Y.; Chen, S.C.; Shih, C.C.; Tsai, W.W.; Chen, H.C.; Kei, C.C.; Chou, T.T.; et al. Wide-Range and Area-Selective Threshold Voltage Tunability in Ultrathin Indium Oxide Transistors. *Nat. Commun.* **2023**, *14*, 10–17. [CrossRef]
6. Yoon, M. Analyzing Transfer Characteristics of Disordered Polymer Field-Effect Transistors for Intrinsic Device Parameter Extraction. *Crystals* **2023**, *13*, 1075. [CrossRef]
7. Yoon, M.; Lee, J. Charge Transfer Doping with an Organic Layer to Achieve a High-Performance p-Type WSe_2 transistor. *J. Mater. Chem. C* **2021**, *9*, 9592–9598. [CrossRef]
8. Nagata, T.; Oh, S.; Yamashita, Y.; Yoshikawa, H.; Ikeno, N.; Kobayashi, K.; Chikyow, T.; Wakayama, Y. Photoelectron Spectroscopic Study of Band Alignment of Polymer/ZnO Photovoltaic Device Structure. *Appl. Phys. Lett.* **2013**, *102*, 043302. [CrossRef]
9. Chiu, F.C.; Chiang, W.P. Trap Exploration in Amorphous Boron-Doped ZnO Films. *Materials* **2015**, *8*, 5795–5805. [CrossRef]
10. Harun, K.; Salleh, N.A.; Deghfel, B.; Yaakob, M.K.; Mohamad, A.A. DFT + U Calculations for Electronic, Structural, and Optical Properties of ZnO Wurtzite Structure: A Review. *Results Phys.* **2020**, *16*, 102829. [CrossRef]
11. Jan, T.; Azmat, S.; Rahman, A.U.; Ilyas, S.Z.; Mehmood, A. Experimental and DFT Study of Al Doped ZnO Nanoparticles with Enhanced Antibacterial Activity. *Ceram. Int.* **2022**, *48*, 20838–20847. [CrossRef]
12. Lee, K.; Ko, G.; Lee, G.H.; Han, G.B.; Sung, M.M.; Ha, T.W.; Kim, J.H.; Im, S. Density of Trap States Measured by Photon Probe into ZnO Based Thin-Film Transistors. *Appl. Phys. Lett.* **2010**, *97*, 082110. [CrossRef]
13. Dhara, S.; Niang, K.M.; Flewitt, A.J.; Nathan, A.; Lynch, S.A. Photoconductive Laser Spectroscopy as a Method to Enhance Defect Spectral Signatures in Amorphous Oxide Semiconductor Thin-Film Transistors. *Appl. Phys. Lett.* **2019**, *114*, 011907. [CrossRef]
14. Kalb, W.L.; Batlogg, B. Calculating the Trap Density of States in Organic Field-Effect Transistors from Experiment: A Comparison of Different Methods. *Phys. Rev. B Condens. Matter Mater. Phys.* **2010**, *81*, 035327. [CrossRef]
15. Kim, S.; Ha, T.J.; Sonar, P.; Dodabalapur, A. Density of Trap States in a Polymer Field-Effect Transistor. *Appl. Phys. Lett.* **2014**, *105*, 133302. [CrossRef]
16. George, S.M. Atomic Layer Deposition: An Overview. *Chem. Rev.* **2010**, *110*, 111–131. [CrossRef]
17. Yoon, M.; Lee, J. Intrinsic Device Parameter Extraction Method for Zinc Oxide-Based Thin-Film Transistors. *Appl. Phys. Express* **2021**, *14*, 124003. [CrossRef]
18. Yoon, M.; Park, J.; Tran, D.C.; Sung, M.M. Fermi-Level Engineering of Atomic Layer-Deposited Zinc Oxide Thin Films for a Vertically Stacked Inverter. *ACS Appl. Electron. Mater.* **2020**, *2*, 537–544. [CrossRef]
19. Yoon, M. Threshold-Voltage Extraction Methods for Atomically Deposited Disordered ZnO Thin-Film Transistors. *Materials* **2023**, *16*, 2940. [CrossRef]
20. Janotti, A.; Van De Walle, C.G. Fundamentals of Zinc Oxide as a Semiconductor. *Rep. Prog. Phys.* **2009**, *72*, 126501. [CrossRef]
21. Huang, Y.L.; Chiu, S.P.; Zhu, Z.X.; Li, Z.Q.; Lin, J.J. Variable-Range-Hopping Conduction Processes in Oxygen Deficient Polycrystalline ZnO Films. *J. Appl. Phys.* **2010**, *107*, 063715. [CrossRef]
22. Wang, W.; Xu, G.; Chowdhury, M.D.H.; Wang, H.; Um, J.K.; Ji, Z.; Gao, N.; Zong, Z.; Bi, C.; Lu, C.; et al. Electric Field Modified Arrhenius Description of Charge Transport in Amorphous Oxide Semiconductor Thin Film Transistors. *Phys. Rev. B* **2018**, *98*, 245308. [CrossRef]
23. Irsigler, P.; Wagner, D.; Dunstan, D.J. On the Application of the Meyer-Neldel Rule to a-Si:H. *J. Phys. C Solid State Phys.* **1983**, *16*, 6605–6613. [CrossRef]
24. Joshi, N.; da Silva, L.F.; Shimizu, F.M.; Mastelaro, V.R.; M'Peko, J.C.; Lin, L.; Oliveira, O.N. UV-Assisted Chemiresistors Made with Gold-Modified ZnO Nanorods to Detect Ozone Gas at Room Temperature. *Microchim. Acta* **2019**, *186*, 418. [CrossRef] [PubMed]
25. Chen, T.; Liu, S.Y.; Xie, Q.; Detavernier, C.; Van Meirhaeghe, R.L.; Qu, X.P. The Effects of Deposition Temperature and Ambient on the Physical and Electrical Performance of DC-Sputtered n-ZnO/p-Si Heterojunction. *Appl. Phys. A Mater. Sci. Process.* **2010**, *98*, 357–365. [CrossRef]
26. Wang, Y.; Kang, K.M.; Kim, M.; Park, H.H. Effective Oxygen-Defect Passivation in Zno Thin Films Prepared by Atomic Layer Deposition Using Hydrogen Peroxide. *J. Korean Ceram. Soc.* **2019**, *56*, 302–307. [CrossRef]
27. Cervantes-López, J.L.; Rangel, R.; Espino, J.; Martínez, E.; García-Gutiérrez, R.; Bartolo-Pérez, P.; Alvarado-Gil, J.J.; Contreras, O.E. Photoluminescence on Cerium-Doped ZnO Nanorods Produced under Sequential Atomic Layer Deposition–Hydrothermal Processes. *Appl. Phys. A Mater. Sci. Process.* **2017**, *123*, 86. [CrossRef]
28. Meijer, E.J.; Matters, M.; Herwig, P.T.; De Leeuw, D.M.; Klapwijk, T.M. The Meyer-Neldel Rule in Organic Thin-Film Transistors. *Appl. Phys. Lett.* **2000**, *76*, 3433–3435. [CrossRef]

29. Dalvi, A.; Parvathala Reddy, N.; Agarwal, S.C. The Meyer-Neldel Rule and Hopping Conduction. *Solid State Commun.* **2012**, *152*, 612–615. [CrossRef]
30. Iñiguez, B.; Nathan, A.; Kloes, A.; Bonnassieux, Y.; Romanjek, K.; Charbonneau, M.; Van Der Steen, J.L.; Gelinck, G.; Gneiting, T.; Mohamed, F.; et al. New Compact Modeling Solutions for Organic and Amorphous Oxide TFTs. *IEEE J. Electron Devices Soc.* **2021**, *9*, 911–932. [CrossRef]
31. Kim, H.; Ng, T.N. Reducing Trap States in Printed Indium Zinc Oxide Transistors by Doping with Benzyl Viologen. *Adv. Electron. Mater.* **2018**, *4*, 2–6. [CrossRef]
32. Lee, S.; Ghaffarzadeh, K.; Nathan, A.; Robertson, J.; Jeon, S.; Kim, C.; Song, I.H.; Chung, U.I. Trap-Limited and Percolation Conduction Mechanisms in Amorphous Oxide Semiconductor Thin Film Transistors. *Appl. Phys. Lett.* **2011**, *98*, 203508. [CrossRef]
33. Upadhyaya, M.; Boyle, C.J.; Venkataraman, D.; Aksamija, Z. Effects of Disorder on Thermoelectric Properties of Semiconducting Polymers. *Sci. Rep.* **2019**, *9*, 5820. [CrossRef] [PubMed]
34. Devkota, S.; Kuzior, B.M.; Karpov, V.G.; Georgiev, D.G.; Li, F.; Borra, V. Percolation Nature of Threshold Switching: An Experimental Verification. In Proceedings of the 2023 IEEE 23rd International Conference on Nanotechnology (NANO), Jeju City, Republic of Korea, 2–5 July 2023; pp. 286–290.
35. Devkota, S.; Nyako, K.A.O.; Kuzior, B.; Karpov, V.; Georgiev, D.G.; Li, F.; Cortes, P.; Borra, V. Threshold Switching in CdTe Photovoltaics. *ECS Meet. Abstr.* **2022**, *109*, 831. [CrossRef]
36. Itapu, S.; Borra, V.; Mossayebi, F. A Computational Study on the Variation of Bandgap Due to Native Defects in Non-Stoichiometric Nio and Pd, Pt Doping in Stoichiometric Nio. *Condens. Matter* **2018**, *3*, 46. [CrossRef]